STAR Protocols

CellPress
OPEN ACCESS

Protocol

Quantitative Imaging of MS2-Tagged hTR in Cajal Bodies: Photobleaching and Photoactivation

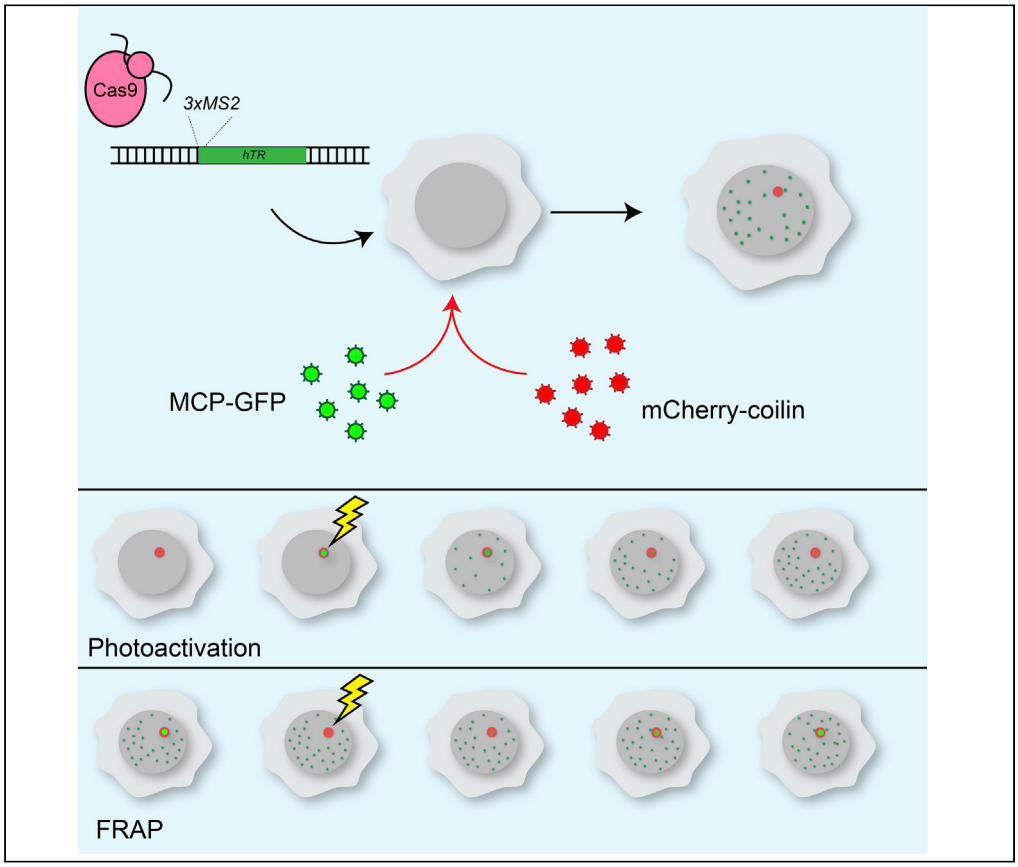

Advances in imaging technologies, gene editing, and fluorescent molecule development have made real-time imaging of nucleic acids practical. Here, we detail methods for imaging the human telomerase RNA template, hTR via the use of three inserted MS2 stem loops and cognate MS2 coat protein (MCP) tagged with superfolder GFP or photoactivatable GFP. These technologies enable tracking of the dynamics of RNA species through Cajal bodies and offer insight into their residence time in Cajal bodies through photobleaching and photoactivation experiments.

Michael Smith, Emmanuelle Querido, Pascal Chartrand, Agnel Sfeir

p.chartrand@umontreal.ca (P.C.)
agnel.sfeir@nyulangone.org (A.S.)

HIGHLIGHTS

Live-cell imaging allows visualization of telomerase RNA at the Cajal body in real time

FRAP analysis is useful for measuring entry of telomerase RNA into the Cajal body

Photoactivation analysis permits measurement of exit dynamics from the same structures

Culture conditions, analysis, and live-cell imaging considerations are detailed

Smith et al., STAR Protocols 1, 100112
December 18, 2020
https://doi.org/10.1016/j.xpro.2020.100112

STAR Protocols

CellPress
OPEN ACCESS

Protocol

Quantitative Imaging of MS2-Tagged hTR in Cajal Bodies: Photobleaching and Photoactivation

Michael Smith,[1,3,4] Emmanuelle Querido,[2,3,4] Pascal Chartrand,[2,*] and Agnel Sfeir[1,5,*]

[1]Skirball Institute of Biomolecular Medicine, Department of Cell Biology, NYU Grossman School of Medicine, New York, NY 10016, USA

[2]Department of Biochemistry and Molecular Medicine, Université de Montréal, Montréal, Canada

[3]These authors contributed equally

[4]Technical Contact

[5]Lead Contact

*Correspondence: p.chartrand@umontreal.ca (P.C.), agnel.sfeir@nyulangone.org (A.S.)
https://doi.org/10.1016/j.xpro.2020.100112

SUMMARY

Advances in imaging technologies, gene editing, and fluorescent molecule development have made real-time imaging of nucleic acids practical. Here, we detail methods for imaging the human telomerase RNA template, hTR via the use of three inserted MS2 stem loops and cognate MS2 coat protein (MCP) tagged with superfolder GFP or photoactivatable GFP. These technologies enable tracking of the dynamics of RNA species through Cajal bodies and offer insight into their residence time in Cajal bodies through photobleaching and photoactivation experiments.

For complete details on the use and execution of this protocol, please refer to Laprade et al. (2020).

BEFORE YOU BEGIN

To image telomerase RNA in live cells, our method makes use of the MS2 tagging system (Bertrand et al., 1998) which allows imaging of RNA indirectly via binding of the GFP-tagged MS2 coat protein (MCP) to MS2 stem loops inserted in the RNA sequence. Since the MS2 coat protein has a very high affinity and very slow off-rate upon binding the MS2 stem-loop (Boireau et al., 2007), this assay is amenable to photoactivation and photobleaching experiments to track the dynamics of the labeled RNA. We have introduced MS2 stem loops into the TERC locus in HeLa 1.3 cells using CRISPR-Cas9 gene editing (referred to as $hTR^{5'MS2}$), an approach detailed in the accompanying manuscript (Laprade et al., 2020). Using both fluorescence recovery after photobleaching (FRAP) as well as photoactivation experiments, we uncovered the dynamic behavior of hTR with respect to Cajal bodies, including its residence time and its recruitment to the specialized bodies. By measuring the decay of activated paGFP over time, we revealed that hTERT controls the dynamic exit of hTR from Cajal bodies. By using FRAP, we measured the half-time of recovery of hTR molecules to the Cajal body. FRAP and photoactivation are complementary strategies and can provide useful insights into how RNAs are loaded to structures such as the Cajal body.

Below, we highlight key steps and some considerations necessary to optimize the microscopy setup for photobleaching and photoactivation experiments. It is important to consider these steps when determining the experimental protocol. Microscopy setups differ widely between laboratories, thus optimization for one's own particular system is necessary.

Integration of MS2 Stem Loops and Selection of Fluorophores

To study the tagged RNA in endogenous expression conditions, stable cell lines containing the modified RNA locus must be developed. In the case of telomerase hTR tagging, we generated

cell lines with three MS2 stem loops inserted into the endogenous hTR locus by CRISPR/Cas9 targeting.

For messenger RNAs, the 3′UTR region is usually chosen to integrate the tag stem loops. To tag non-coding RNAs however, the number and position of MS2 stem loops should be carefully considered because of the need to preserve both RNA localization and function.

For the MS2 system, careful selection of the appropriate fluorophore attached to the MS2 coat protein is essential. The use of databases such as FPbase (Lambert, 2019) can greatly aid in selecting fluorescent molecules.

> *Note:* Absolute measures of fluorescence intensity for various fluorophores marked by databases can be useful, but performance will vary according to cell type and biological contexts. It is important to test novel fluorophores against a known working molecule in specific experimental system to ascertain their individual utility. Tagging a ubiquitous protein such as H2B can also be useful to objectively compare different fluorophores.

For this study, we employed superfolder GFP (Pedelacq et al., 2006), due to its faster maturation time, but the particular experimental system may necessitate different molecules. We generated lentiviral plasmid expressing MS2 coat protein fused to superfolder GFP (MCP-GFP) and introduced them into cells using lentiviral infection.

Lentiviral Infection and Cell Sorting of MCP-GFP for Single-Molecule Imaging of hTR Tagged with MS2 Stem Loops

To infect cells with the proper quantity of MCP-GFP lentivirus so that single molecules of hTR^{5MS2} can be observed with low background, it is necessary to test different concentrations of lentivirus for infection. To prepare high titer lentivirus stock, we use jetPRIME transfection reagent (Polyplus) to introduce 3 μg of lentiviral MCP-GFP plasmid along with 2 μg of gag-pol-rev plasmid (similar to Addgene #8455) and 1 μg of VSVG plasmid (similar to Addgene #8454) on each 10 cm plate of 293FT packaging cells. We collect the 293FT supernatant at 48 h post-transfection, dilute 1/2, 1/8, 1/15, 1/30, or 1/60 in sterile tubes with complete media, and complement with 8 μg/mL polybrene before infection. The five cell cultures infected with the dilutions of MCP-GFP lentivirus are amplified at least two days prior to imaging. MCP-GFP levels are considered adequate when individual particles of hTR are visible and readily detectable by particle tracking software. With this method, users can expect one of the lentiviral dilutions will result in about 10% of cells with adequate signal-to-noise ratio for imaging hTR. To increase this proportion, we recommend sorting the cells for MCP-GFP with a fluorescence activated cell sorter (FACS) as shown in Figure 1. In the following figure, the cells obtained with the A gate were the most suitable for imaging. See Figure 2 for an example of adequate MCP-GFP levels in live cells.

⚠ CRITICAL: infect cells that do not express MS2 tagged-nucleic acids with MCP-GFP lentivirus and image them as a negative control.

Culturing Cells for Live-Cell Imaging

Standard cell culture protocols are followed for the HeLa cells used in these experiments. Prior to imaging, cells are detached from the culture dish and transferred to glass-bottom dishes (#1.5 35 mm dishes from MatTek). Standard culture media may be insufficient for live-cell imaging. Common culture reagents, such as phenol red, add significant background to samples and should be avoided if possible. Therefore, we used a media recipe of phenol red free, glucose supplemented DMEM, with penstrep, 10% BCS/FBS, GLUTAMAX supplement, and 25 mM HEPES pH 7.4. HEPES is added to supplement the carbonate buffering system of the media. If CO_2 is supplied by a microscope incubator, HEPES may be omitted, as using both may lead to media acidification. Microscope culture conditions may require frequent exchanging of plates, so prepare several replicates.

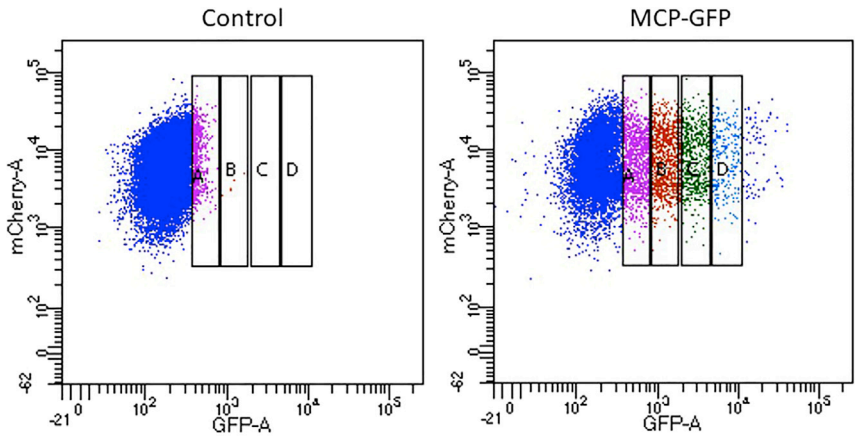

Figure 1. Sorting Profile of Cells Expressing Different Levels of MCP-GFP

Gates were defined on mCherry versus GFP fluorescence. Control cells expressing only mCherry-TRF1 and mCherry-CDT1 versus cells also infected with MCP-GFP at 1/60 dilution. Four gates labeled A, B, C, and D were defined, and the four cell populations were allowed to recover for 5 days before imaging. Population A worked best for single-molecule imaging of MCP-GFP. A FACS Aria III cytometer was used for sorting.

⚠ CRITICAL: It is imperative to test live-cell imaging setup carefully in order to minimize evaporation and pH changes, and to ensure temperature stability. Evaporation and pH can be assessed by monitoring the media before and after a typical experiment, while the temperature is monitoried by introducing a live temperature probe. If evaporation occurs, changes in osmotic pressure in the media can negatively influence cell health, and the chamber should be humidified. pH changes imply improper buffering, and CO_2 levels or HEPES may be inadequate. Temperature fluctuations are indicative of improper heating. This may result from an improperly sealed incubator chamber or in the case that the lens acts as a heat sink, in which case objective lens heating should be considered.

Choosing an Imaging Modality

For our study, we used spinning disk confocal microscopy for optical sectioning and speed. hTR particles are dim and fast moving, thus to visualize them it is essential to minimize out of focus signal through the confocal effect. In addition, it is important to use a system with the capability of rapid image acquisition like an EMCCD camera, which would be more difficult on a point-scanning confocal.

KEY RESOURCES TABLE

REAGENT or RESOURCE	SOURCE	IDENTIFIER
Experimental Models: Cell Lines		
HeLa 1.3 (HeLa 1.2.11 clone 1.3)	De Lange Laboratory, Rockefeller University	N/A
HeLa 1.3 hTR-5′-3xMS2	Laprade et al. 2020	N/A
293FT	ThermoFisher Scientific	R70007
Recombinant DNA		
pHAGE2-UBC-MS2-sfGFP (MCP-GFP)	Laprade et al. 2020	N/A
pHAGE2-UBC-MS2-paGFP (MCP-paGFP)	Laprade et al. 2020	N/A
pHAGE2-EF1a-mCherry-hCoilin-IRES-Hygro	Laprade et al. 2020	N/A

(*Continued on next page*)

Continued

REAGENT or RESOURCE	SOURCE	IDENTIFIER
pCMV-deltaR8.2	Addgene	8455
pCMV-VSV-G	Addgene	8454
Software and Algorithms		
ImageJ v1.52p	Schneider et al., 2012	https://imagej.net
GraphPad Prism version 8	GraphPad	https://www.graphpad.com/scientific-software/prism/
FRAP Profiler	Hardin, 2018	http://worms.zoology.wisc.edu/research/4d/4d.html
Other		
TetraSpeck™ Microspheres, 0.1 μm	ThermoFisher Scientific	T7279
GlutaMAX supplement	ThermoFisher Scientific	35050061
jetPRIME transfection reagent	Polyplus	114-15
Polybrene (Hexadimethrine bromide)	Sigma Aldrich	H9268
Fluorescein sodium salt	Sigma Aldrich	F2456
35 mm Dish No. 1.5 Coverslip	MatTek Life Sciences	P35G-1.5-14-C
FluoroDish cell culture dish 35 mm	World Precision Instruments	FD35-100

STEP-BY-STEP METHOD DETAILS

FRAP Analysis of hTR Foci at Cajal Bodies

Timing: Collecting sufficient cells may take several imaging sessions (of 3–4 h each), analysis may take several days

Below is a basic protocol for FRAP of hTR molecules at Cajal bodies.

1. Plate cells on imaging plates (MatTek) the night before the experiment. In the morning, change media to a live-cell imaging mixture and allow cells to equilibrate for an hour or more.
2. In the meantime, turn on the stage-top incubator (Tokai Hit), allow the temperature to stabilize at 37°C, and fill the attached water bath with sterile ddH_2O. Turn on CO_2 gas as needed.
3. While waiting, take images of TetraSpeck beads (Invitrogen) to use as a channel registration reference (see below).
4. Take 20–30 flat field correction slide images (see below).
5. After cells have equilibrated, move the dish to the stage-top incubator, attach the temperature probe and allow the media to come to 37°C.
6. Focus on cells using brightfield channel, then switch to dual camera mode. We use a Nikon Ti2 Eclipse with a CSU-W1 confocal unit and a Brukker FRAP module. We image Cajal bodies (CBs) using mCherry-coilin (excitation 561 nm) and hTR (488 nm) using MCP-GFP. Dual camera mode (two Andor iXon Life 888 EMCCD cameras connected by a Cairn Dual Emission Image Splitter) allows simultaneous imaging of both structures and allows us to correct or exclude images for analysis in which the CB moves during acquisition. Single-camera images of the mCherry-coilin channel could also be used to define FRAP regions, but CBs are dynamic structures.
7. Identify cells where strong hTR signal visibly colocalizes with CBs. These cells are somewhat rare. When searching for appropriate cells, do not use live camera mode as this leads to bleaching and phototoxicity, as well as inaccurate measurements. Use the lowest illumination possible and take single images using the snap shot function until a desired cell is located.
8. Define a 2 μm circle around the CB using the FRAP software (in our case, Nikon Elements) and bleach using the Brukker galvo system. Some software setups allow imaging through the bleaching process or imaging strictly limited until after the bleach. We image after the bleach, which

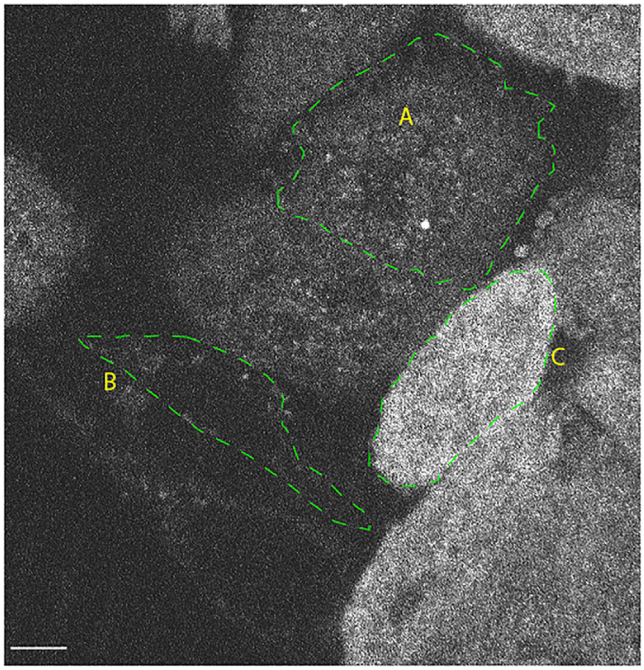

Figure 2. Levels of MCP-GFP Obtained after Lentiviral Infection and FACS Sorting

Cells expressing good (A), excessive (C), and no (B) MCP-GFP, individual cells outlined with green dashed line. Infection with MCP-GFP expressing lentivirus should be titrated to optimize the amount of A cells in the given population. This greatly aids the speed of data acquisition. Scale bar, 6 μm.

entails a short delay, which can be consequential for very fast recoveries. However, imaging the pulse can damage the camera, especially when EM gain is used. For bleaching, we use a 405 nm pulse at low laser power (5%) and with a pixel scan speed of 25 μs per pixel (in total 23.78 ms for a diameter 2 μm circle). The bleach should be sufficiently powerful to remove about 80% or more of the fluorescence before recovery.

9. Bleach and image for 1 min, with 600 ms intervals and 100 ms exposure time. Several pre-bleach images must be taken to determine the baseline fluorescence. We took five such images, at a rate of 1/s.
10. To test for phototoxicity, acquire images of the bleached and imaged cell in a transmitted light channel every 5 to 10 min as necessary. Gross morphological changes should not occur, particularly blebbing of membranes and fragmentation of the cell. This does not need to be repeated for every cell, but should be determined prior to a large-scale experiment.

⚠ CRITICAL: The total amount of images, laser power, and exposure time should be set to maximize SNR, minimize phototoxicity, and minimize acquisition photobleaching (see Troubleshooting). The intensity of a non-FRAP reference region in the cell should not decrease more than 20% of its initial intensity over the course of the imaging (see below). Phototoxicity should be minimized as much as possible (see Troubleshooting).

11. Collect cells as necessary for the experiment. A small-scale pilot experiment with the conditions of interest and a statistical power analysis (for the statistical test intended for the analysis) will guide the total number of cells necessary to identify changes in half-life and mobile fraction between those conditions. The estimated sample size of the full experiment may also be used to determine whether the FRAP protocol is time efficient.

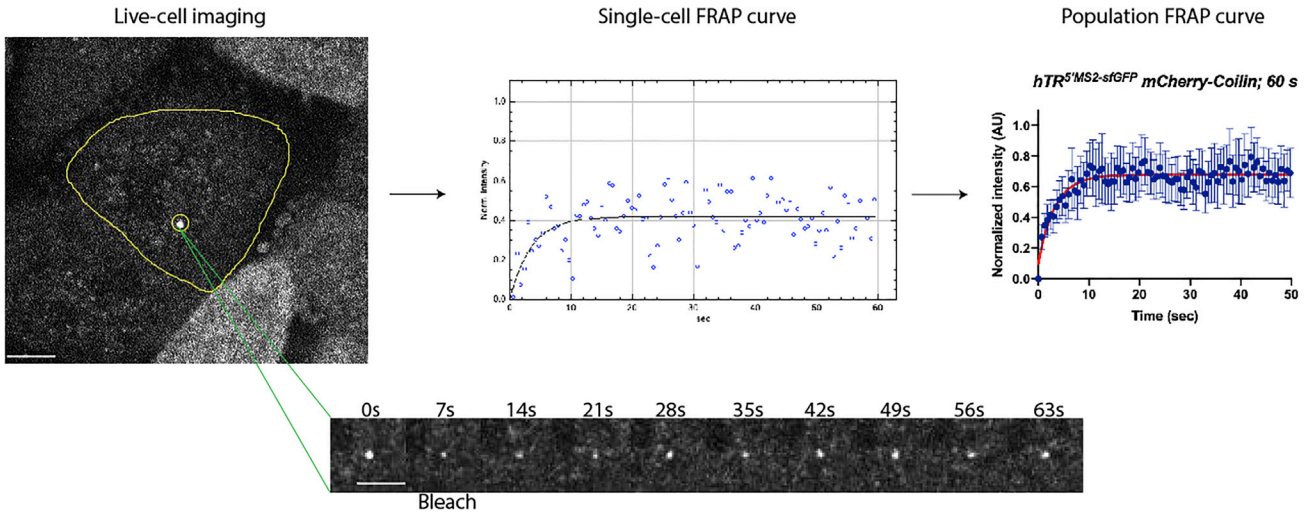

Figure 3. FRAP Analysis Workflow

Individual cells with good FRAP recovery at CBs are identified. The cell and FRAP circle (2 μm) are outlined and the FRAPProfiler plugin in run. Individual FRAP curves are transferred to Prism, averaged, and then fit. From the one-phase association curves, half-life and plateau are extracted. Inset: Photobleach and recovery of CB localized hTR. Scale bar, 6 μm.

Photoactivation of hTR at Cajal Bodies

Timing: Collecting sufficient cells may take several imaging sessions (of 3–4 h each), analysis may take several days

Photoactivation is performed with several differences as detailed below. These experiments were performed on a different spinning disk setup than above. For photoactivation studies, a photoactivatable GFP variant is fused to the MS2 coat protein (MCP-paGFP). This protein increases 100-fold (Patterson and Lippincott-Schwartz, 2002) in fluorescence after a pulse with a 405 nm laser, and the decay of that fluorescence can be recorded over time as a measure of outward migration of labeled molecules from the CB.

12. For these experiments, cells expressing mCherry-coilin and MCP-paGFP are plated on glass-bottom 35 mm dishes (in this case, Fluorodish WPI) and placed in live-cell imaging media as above.
13. Cells are imaged on a Zeiss Axio-Observer Z1 Yokogawa CSU-X1 spinning disk inverted confocal microscope with a 37°C, 5% CO_2 imaging chamber. The lasers (405 nm 50 mW OPSL, 488 nm 100 mW diode, and 561 nm 40 mW diode) should be on for a minimum of 1 h before imaging to stabilize. For photoactivation studies we image Cajal bodies (CBs) using mCherry-coilin (excitation 561 nm) and hTR (488 nm) using MCP-paGFP, sequentially on a single EMCCD camera (Photometrics Evolve 512).
14. The Cajal body defined with mCherry-coilin is positioned in the center of the field of view in Live mode so that it can be targeted by the centered 1.5 μm diameter target area of the Zeiss Direct-FRAP module.
15. Five pre-bleach images of MCP-paGFP are acquired to establish the initial conditions. The exposure time used for MCP-paGFP is 150 ms with an added 30 ms camera transfer time resulting in a 180 ms interval between images. The 1.5 μm target area is exposed to the 405 nm laser (at 20% power) for 500 ms, and 195 images are then acquired to follow the MCP-paGFP signal for a total of 35 s. There is only a 20 ms delay between the end of the 405 nm pulse and the first post-photoactivation exposure. A representative photoactivation experiment is shown in Figure 4A.

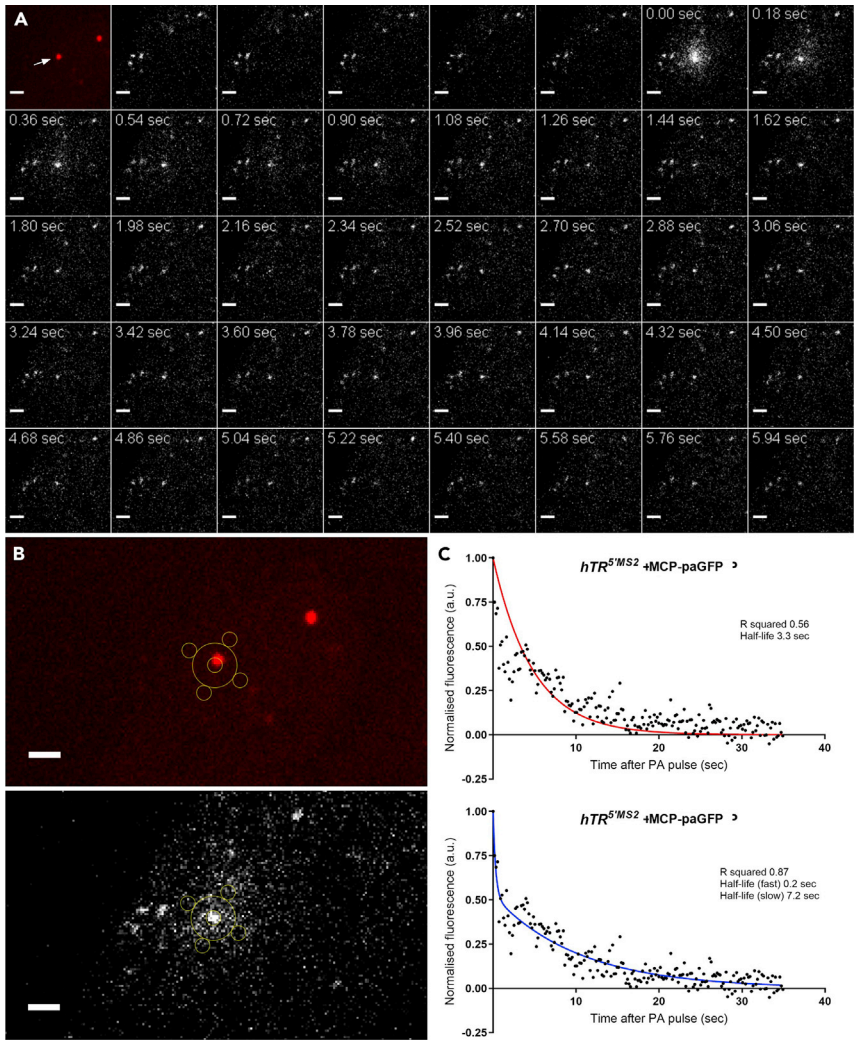

Figure 4. Photoactivation Example and Analysis

(A) Montage of a photoactivation (PA) experiment. The CB targeted with the 405 nm pulse is indicated by an arrow in the red mCherry-coilin image. Five images pre-pulse, followed by 27 images post-PA. The time is indicated for the images after PA.

(B) Positioning of the five measurement regions for PA image analysis. mCherry-coilin image in red and MCP-paGFP below in gray.

(C) Choice of equation for quantitation of photactivation curves to account for bound and unbound MCP-paGFP fractions. GraphPad Prism one-phase exponential decay curve on top in red compared to two-phase exponential decay curve in blue below. Scale bars, 2 μm.

EXPECTED OUTCOMES

See Figures 3 and 4 for examples of ideal results and analysis platforms. Please also see (Laprade et al., 2020) for video examples of these experiments.

The main value to be extracted from FRAP and photoactivation experiments are the half-lives of entry and exit into a given region or structure respectively, although FRAP can also give an estimate of the amount of RNA that is stable within the bleached region (see Analysis below). For Cajal bodies, using our protocol in *hTR*$^{5'MS2}$hTR HeLa 1.3 cells, we observe a half-life of entry into Cajal bodies of 2.3 s, and a mobile fraction of 68%. For photoactivation experiments, we find two populations of exit half-lives with a fast diffusing population (median .6 s) and a slow diffusing population (median 7.5 s).

In this manner, FRAP and photoactivation can be used to explore the entry and exit dynamics of an RNA into a given cellular subdomain and can be used to define a system for further genetic or chemical experiments.

QUANTIFICATION AND STATISTICAL ANALYSIS

Photobleaching and photoactivation studies offer differing types of analytical benefit. For photobleaching, the half-life of recruitment of a given RNA can be determined, as well as the percent of that RNA turned over in the bleached structure during a given length of time (mobile fraction). Recruitment halftimes may differ from exit halftimes, as we found for hTR, so photoactivation experiments can uncover the rate at which RNA molecules exit a certain structure. The two approaches are complementary and can reveal useful data about the dynamics of the RNA in question.

⚠ CRITICAL: Image corrections are essential to analysis of image data. Below, we detail three such corrections (registration, bleedthrough, and flat field correction) that should be used for both FRAP and photoactivation experiments. Images are also background subtracted before analysis to remove camera offset and nonspecific signal.

Photobleaching

Nikon Elements files were imported into FIJI (Schindelin et al., 2012) using Bio-Formats (Linkert et al., 2010). At least two major image corrections must be performed to accurately measure fluorescence recovery. First, channel registration must be verified using 4-color beads, which will show spatial separation between channels. This can be easily corrected in post-processing using the Descriptor-based Registration plugin, and is essential for photobleaching because the red channel (mCherry-coilin) is used to position the bleaching for the green channel (MCP-GFP). Second, inhomogeneity in illumination should be corrected. This is important because many areas of the imaged field do not receive the same illumination as others, and this will cause varying emission behavior. We utilize flat field correction slides as detailed by Model and Burkhardt (2001), and detail the correction method below. These slides are formed by a concentrated fluorescein (or other dye depending on the channel used, in this case the 488 nm channel) solution sandwiched between a slide and coverslip, which causes quenching of fluorescence outside a very thin layer. By averaging images of these slides (20–30 images), subtracting camera noise (average of 10 images with the camera covered or the lasers off), and normalizing, this inhomogeneity can be corrected by dividing out the resultant image from the experimental movies. We use the following method to perform these corrections:

1. Use "Images to Stack" to add all the dark images to a single stack.
2. Use the Z projection function in FIJI to average the images.
3. Use "Images to Stack" to add all the flat field images to a single stack. Use the Z projection function in FIJI to take a median of the images.
4. Use the image calculator function to subtract the noise (dark image average) from the flat field median.
5. Select the resultant image, measure the mean intensity of the entire image, then use the Math option to divide the whole image by that value to normalize the intensity values.
6. Use the image calculator to divide the FRAP movie by this normalized flat field median image. The movie is now corrected for illumination inhomogeneity.

Third, the possibility of channel bleedthrough in the case of using multichannel imaging should be considered and controlled for. Prior to analysis, single-labeled controls can be imaged to assess the level of channel bleedthrough and autofluorescence. These values are then subtracted from the other channels to give a clearer picture of the true fluorescence from a given channel. We provide a method for the correction below:

7. Acquire images for each fluorophore singly in cells. For example, for a cell marked with mCherry-coilin, images should be taken of the GFP channel. In addition, unlabeled cells should be imaged in all channels that will be analyzed as a marker for autofluorescence.
8. For a given channel, perform a colocalization analysis using a plugin such as coloc2 in FIJI. It may be more useful to perform this measurement in a constrained ROI around a structure of interest. For example, to identify the bleedthrough of mCherry-coilin into GFP, perform the analysis between the red and the green channel. The slope of the colocalization correlation curve (Pearson's, for example) can be used to estimate the percent bleedthrough.
9. When performing a FRAP analysis of the MCP-GFP channel, subtract the bleedthrough mCherry signal first. This can be done by duplicating the GFP image, multiplying the duplicated image by the percent bleedthrough determined previously and subtracting the resultant image from the image to be analyzed using the Image Calculator in FIJI. The mCherry-coilin bleedthrough signal has now been approximately removed. The same process can be followed to remove autofluorescence.

⚠ CRITICAL: This post-processing method of bleedthrough correction should only be performed after all sources of bleedthrough/autofluorescence have been reduced experimentally. This can include optimizing filter setups and laser lines as well as removing fluorescent substances (such as phenol red) from the culture medium.

FRAP analysis was performed as described below:

10. Using the FRAP point, draw a 2 μm circle around that point and add it to the ROI manager.
11. Either manually or using image segmentation, draw an ROI around the entire cell as well and add it to the manager.
12. Select the FRAP circle and run the FRAP Profiler plugin (Hardin, 2018). This plugin uses a double-normalization (Phair et al., 2004) method for FRAP analysis, which does not require photobleaching correction, but requires a large reference space as a measure for background.
13. Transfer the data to a spreadsheet.

⚠ CRITICAL: It is important to only analyze cells in which a clear and obvious hTR focus is bleached and then obviously recovers in the time period of interest. This is because cells contain MS2-tagged hTR bound to MCP-GFP as well as free MCP-GFP molecules. Only the tagged RNA foci are of interest, and including recovery of free MCP-GFP may degrade the quality of the analysis. The initial presence and reappearance of the MCP-GFP-tagged hTR focus can be confirmed using particle tracking software such as TrackMate, with the particle tracking parameters defined using the reference images taken before the bleach.

We use GraphPad prism to create FRAP curves via a one-phase association model. The number of cells necessary for proper analysis should be determined via a pilot experiment and an analysis of statistical power for the statistical test intended to be used for the full experiment. We used Student's *t* test to compare the half-lives and mobile fractions from different experimental conditions. This fitting model may not be sufficient for all FRAP recovery curves, and two-phase or other models may be more appropriate for some experiments.

These fitting models can be used to extract the half-time of recovery as well as the value of the curve at its plateau, which expresses the amount of the exchanged RNA during the length of the experiment (mobile fraction). For example, in the FRAP curve shown in Figure 3 (right), the ensemble FRAP curve plateaus at a value around .68, suggesting that the fraction of bleached molecules exchanged with fluorescent molecules during the length of this experiment was around 68%.

Note: Our fitting model assumes first-order photobleaching kinetics and does not account for more complex photobleaching dynamics such as saturation. This can limit the interpretive power of the analysis (Braeckmans et al., 2006).

Photoactivation

14. Zeiss czi files are imported into ImageJ and converted to single channel 16-bit TIFFs. To correct signal loss from acquisition photobleaching, the ImageJ exponential fit bleach correction is applied to the paGFP fluorescence profile.
15. The measurement region is a 7 pixels diameter circle (0.93 μm) centered on the position of the MCP-paGFP foci as shown in Figure 4B. When no MCP-paGFP foci appears after PA, the measurement region is centered on the Cajal body. The fluorescence background of MCP-paGFP is measured in four 7 pixels diameter regions in the nucleoplasm surrounding the Cajal body position.
16. The average background of the four surrounding regions is subtracted from the center value at each time-point. The value of fluorescence in the first image after PA, is set to 1 and all subsequent values are reported as a fraction of 1.
17. The paGFP fluorescence decay curves are analyzed in GraphPad prism with exponential decay equations. The CBs of *hTR*$^{5'MS2}$ cells in which hTR was detected have two populations of MCP-paGFP (free and hTR$^{5'MS2}$ -bound) and are analyzed with the two-phase exponential decay equation as shown in Figure 4C.

LIMITATIONS

Depending on the dynamic behavior of the RNA in question, recovery may not be observed. Also, the physical configuration of the imaging hardware may limit the ability to take images quickly enough to capture fast recoveries. As always, phototoxicity in the observed cell line may make certain experimental configurations difficult, and should be carefully considered and controlled for.

TROUBLESHOOTING

Problem

MCP-GFP foci cannot be visualized.

Potential Solution: Optimize Your System to Increase SNR

MS2-tagged hTR molecules, in general, are quite dim and somewhat difficult to localize. Thus, extracting the highest possible signal-to-noise ratio (SNR) is required for proper analysis of data. Particle tracking software can help determine the necessary SNR, as only particles of sufficient signal are able to be tracked.The main methods for increasing signal-to-noise ratio and enabling particle tracking include minimizing spherical aberration, choosing high quality fluorophores (bright and durable in the cells used), and several steps taken on the microscope used for the experiment. Spherical aberration is an omnipresent issue in light microscopy and can degrade signal, making analysis difficult or impossible. For a more complete review of reducing this issue, see (Ross et al., 2014). In brief, mismatches in refractive index along the light path must be minimized. This can be accomplished by using the proper cover slips (#1.5 is appropriate for most modern lenses, but check slip thickness against the optimal range for the lens in use) and immersion oil, as well as adjusting correction collars on the lenses themselves.

Several factors in the microscopy setup and imaging protocol can increase available signal. These include excitation power, exposure time, choice of camera and lens, and camera gain/EM gain. Modern confocal microscopes include adjustable power laser launches. Naturally, the more light used to excite the sample, the more photons will be emitted. However, cells do not necessarily tolerate high levels of illumination, and it is possible to damage or kill the cells under analysis (see below).

SNR can also be enhanced by longer exposure time. However, if one is interested in rapid motion behaviors, such as the ones we observe for hTR, then the exposure time will be limited by the need for adequate temporal sampling (Waters and Wittmann, 2014). The need for higher SNR will have to be balanced against the characteristics of the phenomena under investigation.

Proper choice of lenses and cameras can greatly affect the ability to observe hTR and other RNAs. In general, the lowest magnification lens with the highest numerical aperture necessary to see the biology of interest should be used. If the numerical aperture of the lens is similar between a 60× and a 100× lens, then the 60× lens will accept more photons and yield higher signal. One consideration in imaging hTR foci is that sufficient axial sampling of the camera setup is necessary to observe single molecules. In other words, magnification should be set such that the structure of interest is observed with a sufficient number of pixels. The exact number will vary but Nyquist sampling is a useful minimum standard. For that reason, we use a 100× lens (Nikon, Plan Apo, 1.35). Sufficient pixel sampling of hTR foci is necessary to visualize them. Cameras should be chosen for high dynamic range and pixel resolution. Larger chips can make acquiring sufficient data more rapid. When visualizing highly dynamic structures, camera speed needs optimization, and may require advance hardware triggering setups to optimize. This was essential to visualize hTR dynamics.

Lastly, many modern cameras incorporate some form of digital gain, which can increase signal. The classic form of camera gain operates by driving higher voltages across the analog to digital converters with the camera's CCD chip. This increases signal at the cost of more noise. EMCCD cameras have a secondary gain function in which electrons produced by photons striking the chip can be amplified via collisions with a silicon element within the camera. The amplification again varies with voltage and can be adjusted (Lambert and Waters, 2014). However, this amplification causes a multiplicative increase in noise, which can limit its utility. Still, for dim hTR particles, EM gain was essential for sufficient SNR.

We detail a simple method for calculating SNR below.

> *Caution:* Microscope software often assigns arbitrary values to sliders for illumination intensity and EMCCD levels. It is thus difficult to provide example ranges for these values, and they should be tested for each experiment by the user. Also beware arbitrary percentage measurements of illumination intensity, which are frequently nonlinear. Another important consideration is that some laser launches do not have consistent power output over time, which can be especially problematic for sensitive FRAP experiments. Stage-top measurement devices can help to assign meaningful real-world values to these numbers and may also help standardize conditions between experiments.

Measuring signal-to-noise ratio

1. In FIJI or similar software, select a structure or region of interest. These values are estimates, so precise segmentation may not be necessary.
2. Measure the intensity of this region, as well as the standard deviation of that intensity. Formally, this value is the noise.
3. Measure the intensity of a region of background.
4. Subtract the background intensity from the object of interest's intensity, and divide by the noise. This ratio can be compared as imaging conditions change, allowing a roughly quantitative measurement of image quality.

Problem

Cells are sick or dying during imaging.

Potential Solution: Minimize Phototoxicity and Improve Culture Conditions

As noted above, light exposure can be toxic to cells (Ettinger and Wittmann, 2014). If cells are visibly blebbing or detaching during imaging as determined by post-experiment transmitted light imaging, reduce the intensity of illumination or minimize exposure times. More troubling is the possibility of subtle effects on morphology and behavior of different structures. Cells should always be tested with different levels of illumination, and gross changes in morphology should be monitored in transmitted light channels at the very least. Post-imaging growth of the cell culture can also be monitored. Analyses performed on dead or stressed cells are not valid, so this concern should be taken seriously.

Culture conditions may also affect cell health. When culturing cells on the microscope, pH, humidity, and temperature must be strictly controlled, or cell health will be negatively affected. We use a Tokai Hit stage-top incubator, but enclosure style models are also available. In the incubator, we use a heated water bath to control humidity, supplemental CO_2 to control pH, and a temperature probe to maintain the media at 37°C. Culture conditions, optimal temperature, and buffering systems may vary between cell lines, so ensure that the system is optimized for the line being used.

RESOURCE AVAILABILITY

Lead Contact

Further information and requests for resources and reagents should be directed to and will be fulfilled by the Lead Contacts, Agnel Sfeir and Pascal Chartrand (agnel.sfeir@nyulangone.org, p.chartrand@umontreal.ca).

Materials Availability

Requests for materials will be fulfilled after execution of a suitable Materials Transfer Agreement. Plasmids generated in this study are available at Addgene.

Data and Code Availability

Imaging data supporting the current study are available from the corresponding author on request.

ACKNOWLEDGMENTS

We would like to thank the members of the Sfeir and Chartrand laboratories for their useful feedback and contributions. We acknowledge the microscopy core at NYU School of Medicine and UdeM. This project was funded by grants from the Hirschl-Weill-Caulier Foundation (A.S.), the Canadian Institutes of Health Research (PJT-162156), and the Canadian Cancer Society Research Institute (CCSRI) to P.C. P.C. holds a research chair from Fonds de Recherche du Québec-Santé (FRQS).

AUTHOR CONTRIBUTIONS

M.J.S. developed the FRAP live-cell imaging methods and analysis. E.Q. developed the cell culture protocols and photoactivation methods and analysis. M.J.S. and E.Q. wrote the manuscript. A.S. and P.C. supervised the work, edited the manuscript, and funded the project.

DECLARATION OF INTERESTS

A.S. is a co-founder of Repare Therapeutics and a member of its scientific advisory board.

REFERENCES

Bertrand, E., Chartrand, P., Schaefer, M., Shenoy, S.M., Singer, R.H., and Long, R.M. (1998). Localization of ASH1 mRNA particles in living yeast. Mol. Cell *2*, 437–445.

Boireau, S., Maiuri, P., Basyuk, E., de la Mata, M., Knezevich, A., Pradet-Balade, B., Backer, V., Kornblihtt, A., Marcello, A., and Bertrand, E. (2007). The transcriptional cycle of HIV-1 in real-time and live cells. J. Cell Biol. *179*, 291–304.

Braeckmans, K., Stubbe, B.G., Remaut, K., Demeester, J., and De Smedt, S.C. (2006). Anomalous photobleaching in fluorescence recovery after photobleaching measurements due to excitation saturation–a case study for fluorescein. J. Biomed. Opt. *11*, 044013.

Ettinger, A., and Wittmann, T. (2014). Fluorescence live cell imaging. Methods Cell Biol. *123*, 77–94.

Hardin, J. (2018). Microscopy, viewed 21 August, 2020. http://worms.zoology.wisc.edu/research/4d/4d.html.

Lambert, T.J. (2019). FPbase: a community-editable fluorescent protein database. Nat. Methods *16*, 277–278.

Lambert, T.J., and Waters, J.C. (2014). Assessing camera performance for quantitative microscopy. Methods Cell Biol. *123*, 35–53.

Laprade, H., Querido, E., Smith, M.J., Guerit, D., Crimmins, H., Conomos, D., Pourret, E., Chartrand, P., and Sfeir, A. (2020). Single-molecule imaging of telomerase RNA reveals a recruitment-retention model for telomere elongation. Mol. Cell *79*, 115–126.e6.

Linkert, M., Rueden, C.T., Allan, C., Burel, J.M., Moore, W., Patterson, A., Loranger, B., Moore, J., Neves, C., Macdonald, D., et al. (2010). Metadata matters: access to image data in the real world. J. Cell Biol. *189*, 777–782.

Model, M.A., and Burkhardt, J.K. (2001). A standard for calibration and shading correction of a fluorescence microscope. Cytometry *44*, 309–316.

Patterson, G.H., and Lippincott-Schwartz, J. (2002). A photoactivatable GFP for selective photolabeling of proteins and cells. Science *297*, 1873–1877.

Pedelacq, J.D., Cabantous, S., Tran, T., Terwilliger, T.C., and Waldo, G.S. (2006). Engineering and characterization of a superfolder green fluorescent protein. Nat. Biotechnol. *24*, 79–88.

Phair, R.D., Gorski, S.A., and Misteli, T. (2004). Measurement of dynamic protein binding to chromatin in vivo, using photobleaching microscopy. Methods Enzymol. *375*, 393–414.

Ross, S.T., Allen, J.R., and Davidson, M.W. (2014). Practical considerations of objective lenses for application in cell biology. Methods Cell Biol. *123*, 19–34.

Schindelin, J., Arganda-Carreras, I., Frise, E., Kaynig, V., Longair, M., Pietzsch, T., Preibisch, S., Rueden, C., Saalfeld, S., Schmid, B., et al. (2012). Fiji: an open-source platform for biological-image analysis. Nat. Methods *9*, 676–682.

Schneider, C.A., Rasband, W.S., and Eliceiri, K.W. (2012). NIH Image to Image J: 25 years of image analysis. Nat. Methods *9*, 671–675.

Waters, J.C., and Wittmann, T. (2014). Concepts in quantitative fluorescence microscopy. Methods Cell Biol. *123*, 1–18.